Aerodynamic Analysis of UAVs. MFD Nimbus

Vasile PRISACARIU*

*Corresponding author
"Henri Coanda" Air Force Academy of Brasov,
160 Mihai Viteazul Street, Brasov 5001833, Romania,
aerosavelli73@yahoo.com

DOI: 10.13111/2066-8201.2019.11.2.11

Received: 23 April 2019/ Accepted: 22 May 2019/ Published: June 2019

Abstract: *The robotic airborne systems have undergone a rapid development due to information requirements with data from areas of interest and technological miniaturization. Although these aerial systems have high capabilities, they are used for specific missions and limited to atmospheric factors. The performance and technical-tactical characteristics of an air vector depend directly on aerodynamics, the reliability of systems and the human factor and on the influence of disruptive factors. At global level, the aerial systems have 6 missions (surveillance, detection, classification, identification, tracking and neutralization) that can be accomplished at different operational levels depending on the aerodynamic and technical tactical features. The article includes a series of flight performance analyses for Nimbus MFD, 2D profile and 3D analysis of the entire aircraft without the interference generated by the propeller.*

Key Words: *aerodynamic analysis, MFD Nimbus, FPV flight, XFLR5*

SYMBOLS AND ACRONYMS

EPO	*Expanded PolyOlefin*	*RC*	*Radio control*
FPV	*First person view*	*AoA*	*Angle of attack*
C_l	*Lift coefficient*	*VLM*	*Vortex Lattice Method*
MAC	*Mean Aerodynamic Chord*	*GMC*	*Mean Geometric Chord*
C_d	*Drag coefficient*	*S*	*Wing Area*
TR	*Taper ratio*	C_m	*Pitch coefficient*
AR	*Aspect ratio*	*V*	*Speed*
L	*lift*	*W*	*Weight*
c_R,c_T	*Root chord / tip chord*	*b*	*Wing span*
x_c	*Chord coordinate*		

1. INTRODUCTION

The robotic airborne system (UAS) contains RC ground equipments and aerial vector (UAV) that use aerodynamic forces to move on the desired, non-ballistic, directed or self-controlled trajectories and which carry payloads, depending on the mission.

Globally, unmanned aerial systems have 5 missions (surveillance, detection, classification, identification and tracking) that can be accomplished at different operational levels according to aerodynamic and tactical tactics.

Nimbus is a MFD (MyFlyDream) aircraft in the UAV concept, electric two motors, rectangular wing placed up and V-tail.

The front detachable fuselage provides space for radio electronic equipment and the rear fuselage is made of carbon tube.

All construction elements are designed modularly for assembly, storage and transport. The materials used are carbon fiber (rear fuselage), EPO foam (wings, fuselage and tails) and plastic and metal (assembly elements), see Figure 1.

Fig. 1 MyFlyDream Nimbus

Due to its flight characteristics (see Table 1), Nimbus can carry out a number of missions as follows: acquisition of telemetry and image data available in the on-board delivery (GPS, autonomy); acquisition of atmospheric data, based on on-board environmental sensors (temperature, humidity); acquisition of data on 3D trajectory behaviour and structural behaviour of sensors on board, [1, 2].

Table 1. Features and flight data, [1, 2]

Feature	**Value**	**Feature**	**Value**
Span / length	1,8 / 1,3 m	Autonomy	1,5 – 2,5 h
Area	0,375 m^2	Propulsion	2x electric 12 V
Max speed	130 km/h	Battery	6S, 16 A
Max weight / payload	5,5 / 1,5 kg	System RC / servo	2,4 GHz, 6 ch / 6
Ceiling	3500 m	Sensor	EO-IR

The following is an aerodynamic analysis of a single geometric configuration (no engine aircraft) based on two configurations: without engine nacelle and two engine nacelle on the main load lifting surface (wing), an analysis that wishes to highlight the differences performance of the two configurations analyzed.

2. PARAMETERS

Starting from the data provided by the manufacturer [1] we can estimate a number of theoretical parameters [7], as follows:
-aspect ratio:

$$AR = \frac{b^2}{S} = 7{,}66 \text{ m}^2 \quad (1)$$

-wing area: S=0,423 m^2, the difference (up to 0.375 m^2) is the overlap with the fuselage.
-tapper ratio:

$$TR = \frac{c_T}{c_R} = 0{,}74 \quad (2)$$

-mean geometrical chord:

$$MGC = \frac{S}{b} = 0{,}23 \text{ m} \quad (3)$$

-mean aerodynamic chord:

$$MAC = \frac{2}{3} \cdot c_R \cdot \frac{1+TR+TR^2}{1+TR} = 0{,}2367 \text{ m} \quad (4)$$

-MAC interval to C_R:

$$y_{MAC} = \frac{b}{6} \cdot \left(\frac{1+2 \cdot TR}{1+TR}\right) = 0{,}4277 \text{ m} \quad (5)$$

-minimum speed for maximum descent ratio AoA=4^0 fot Clark Y, C_{lmax}=0,85:

$$V_{min} = \sqrt{\frac{W}{S} \cdot \frac{2}{\rho} \cdot \frac{1}{C_l}} = 15{,}64 \text{ m/s} \quad (6)$$

-lifting for C_l=0,85 at (AoA=4^0):

$$L = \frac{\rho \cdot V^2}{2} \cdot S \cdot C_l = 5{,}01 \text{ kg} \quad (7)$$

3. GEOMETRIC CONFIGURATION

XFLR5 [3, 8] provides geometric parameterization tools for both the revolutionary bodies (fuselage) and the lifting surfaces (wing, tails). The graphical user interface is intuitive and easy to use, providing both numeric editing areas (see Figure 3b) and graphical and final geometry information (see Figure 3c). For configuration, it was intended to reproduce the NIMBUS geometry at the 1:1 scale with: 2D definition of airfoil wing and tails, definition of 3D wing geometry, fuselage, and tails.

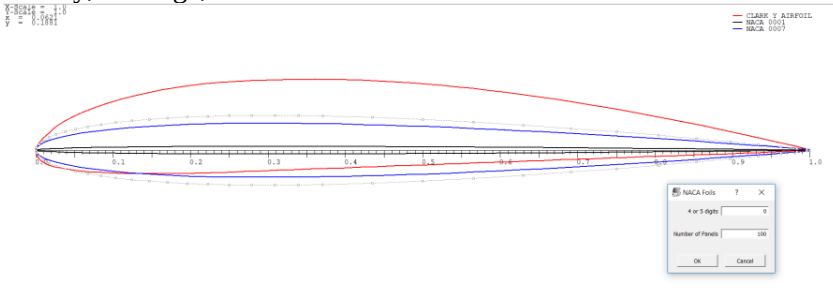

Fig. 2 Airfoils design

The XFLR5 software tool [3] allows both the import of database profiles (external * .dat files) and the definition using a NACA internal editor (see figure 2). Then refine the curve of the profile (maximum 99 segments).

For defining the geometry of the airplane, the geometric phases of the fuselage wing and the tail are shown, see Figure 3.

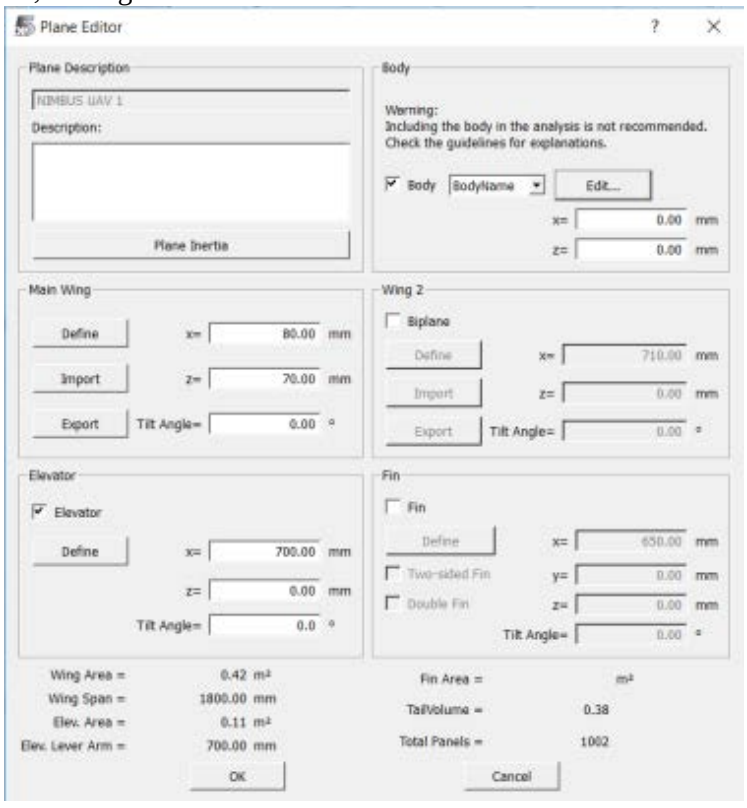

a

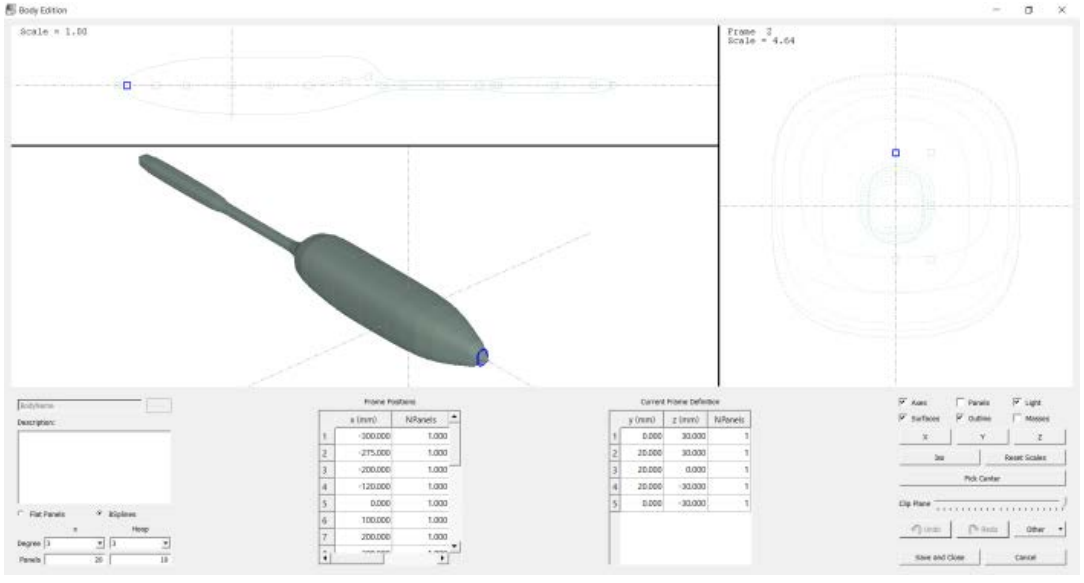

b

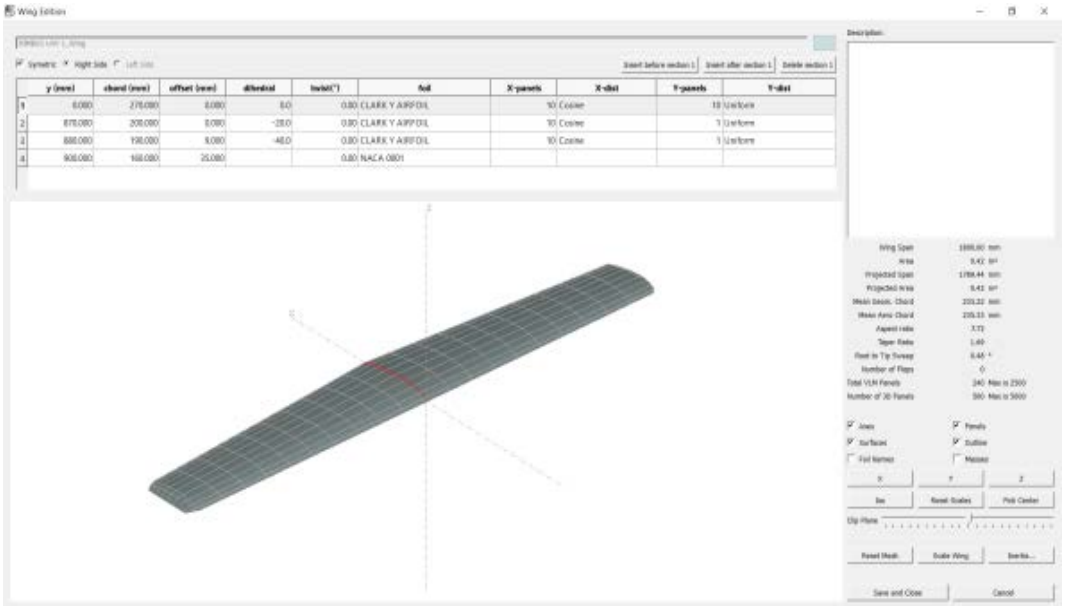

c

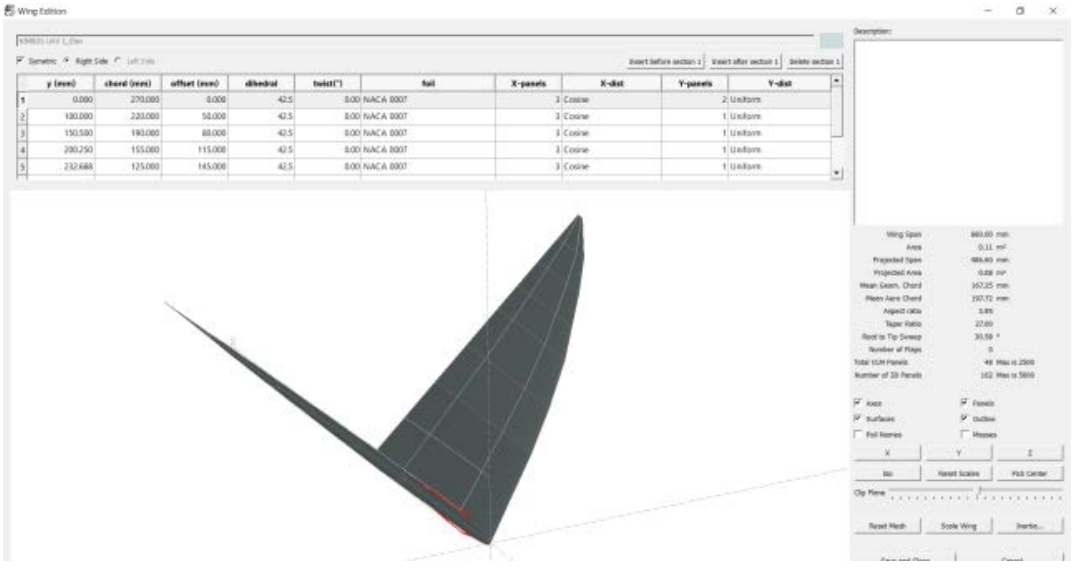

d

Fig. 3 3D geometric steps – MFD Nimbus (a. the main geometric menu, b. fuselaje, c. wing, d. tails)

The virtual assembling of the plane is shown in Figure 4, the relative positioning of the geometric elements is performed in the main geometric menu of Figure 3a.

Achieving the XFLR5 geometry of this plane has a number of limitations on surface connections and the insertion of constructive elements that can influence global aerodynamics (propellers, antennas, and nacelle).

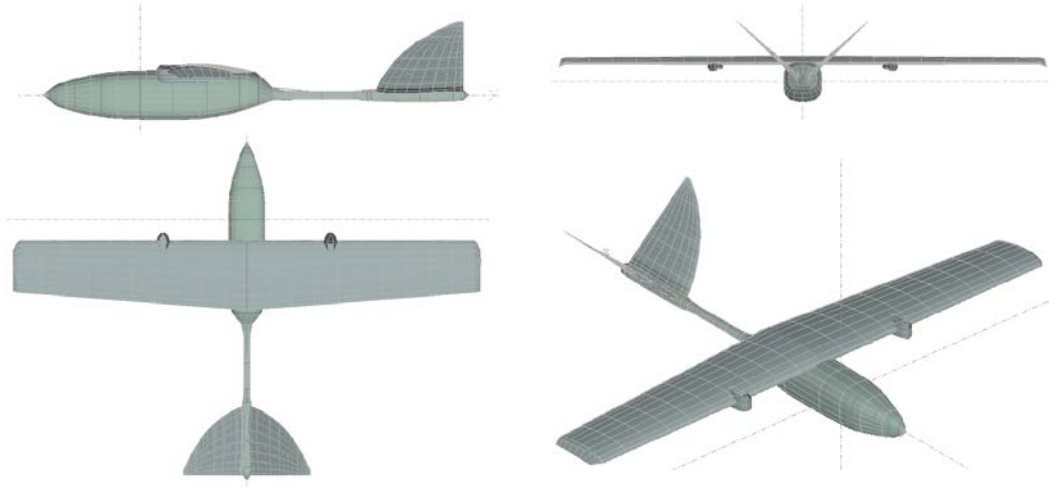

Fig. 4 UAV MFD Nimbus

4. AERODYNAMIC ANALYSIS

Aerodynamic analyses aim at identifying the flight characteristics of this airplane without inertial conditions.

4.1 2D aerodynamic analysis (airfoil)

Cases of aerodynamic analysis include the 2D profile geometry under the conditions of analysis in Table 2.

Table 2. Analysis conditions, [2, 3]

Feature	Value	Feature	Value
Re	$2{,}5 \times 10^5 \div 5 \times 10^5$	Air kinematic viscosity	$1{,}42 \times 10^{-5}$
Iterations	500	AoA	$-5^0 \div 15^0$

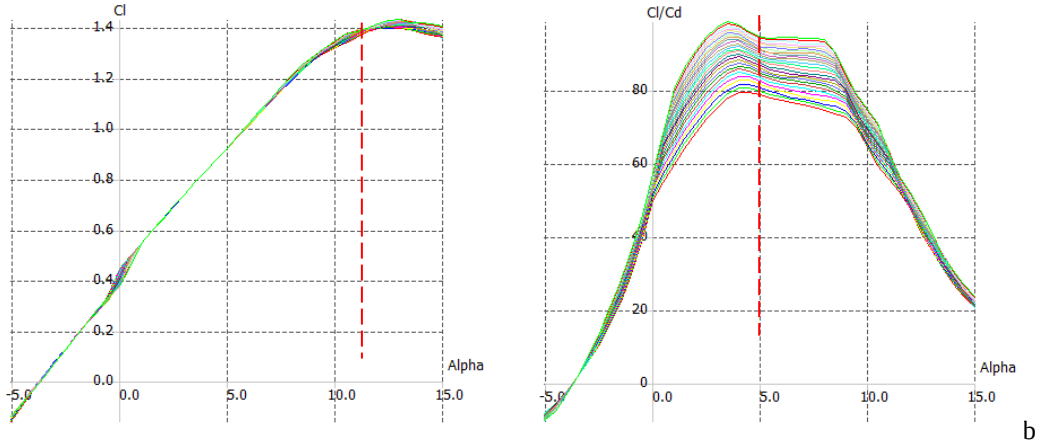

a b

Fig. 5 Clark Y parameters, a. C_l vs AoA, b. C_l/C_d vs AoA

According to online analyses [4] and literature [5, 6, 9, 10, 11, 12], can see similar maximum values of C_l vs AoA and the lift-to-drag ratio of the profile (C_l/C_d vs. AoA) to

AoA=4^0 (figure 5a and 5b). Note that the value of AoA>5^0 for which C_d increases (figure 6a) and the value AoA = 8^0 for the maximum endurance factor (Figure 6.b).

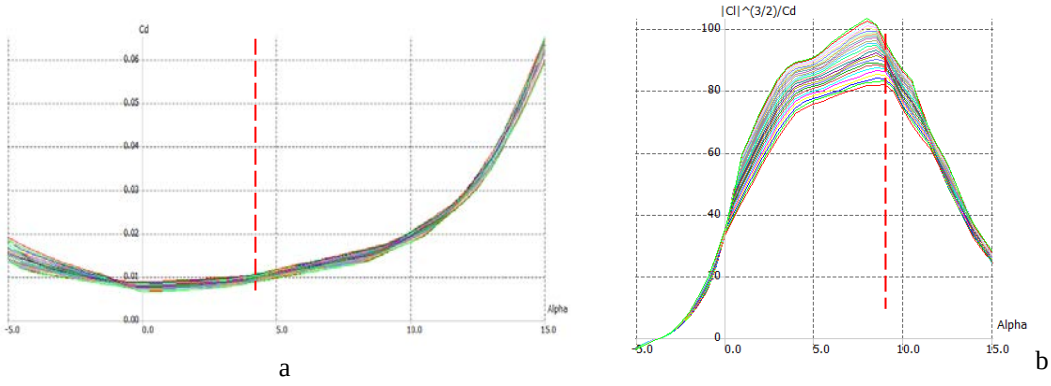

a b

Fig. 6 Clark Y parameters, a. Cl vs Cd, b. $C_l^{(3/2)}/C_d$

Therefore, it is recommended to use an incidence range of 0^o<AoA<5^o for maximum lift-to-drag ratio under the conditions of an optimal C_d.

In Figure 7 we have similar distributions of the pressure coefficient, with the paper [11, 12].

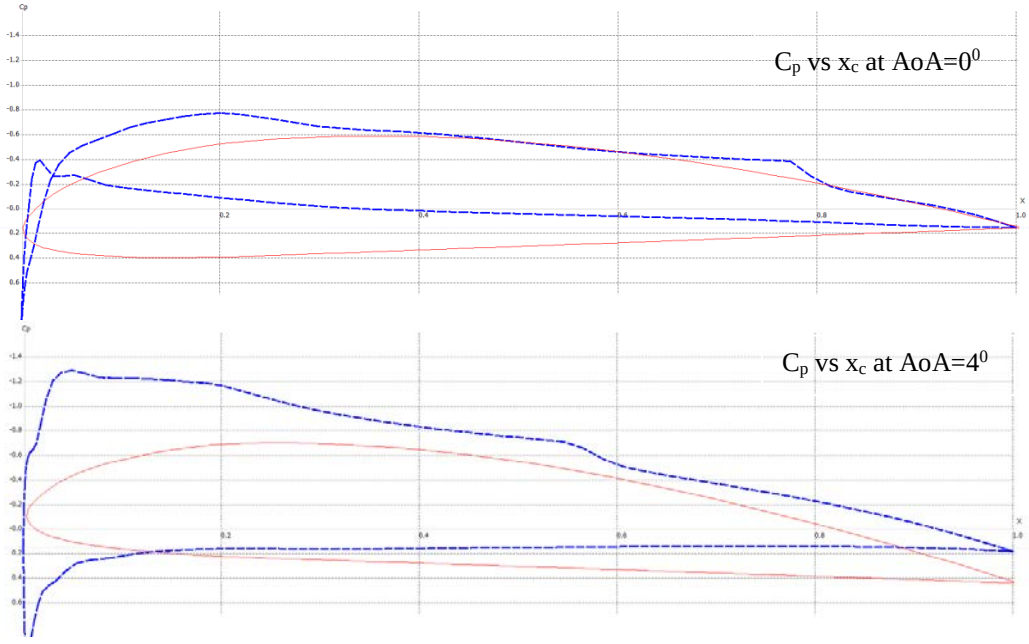

Fig. 7 C_p distribution vs x_c

4.2 3D aerodynamic analyses. Nacelle influence

For 3D aerodynamic analyses, it is proposed to highlight the influence of the presence of electric motor nacelle on aerodynamic performance under the conditions of analysis in Table 3.

Table 3. Analysis conditions, [2, 3]

Feature	Value	Feature	Value
Method analysis	3D panels/VLM	Iterations	100
Tip wing nr. Re	3,84 x 10^5	Root wing nr. Re	6,48 x 10^5
Air density	1,225 kg/m^3	Air kinematic viscosity	1,42 x 10^{-5}
Speed	15 m/s	AoA	$-5^0 \div 15^0$

The aerodynamic analysis set is performed at 15 m/s (theoretical minimum speed). According to Figure 8a, as expected, a negative influence of the presence of motor nacelle on a given C_L value is observed; nacelle influence is also observed in Figure 8b by decreasing C_L to a constant AoA.

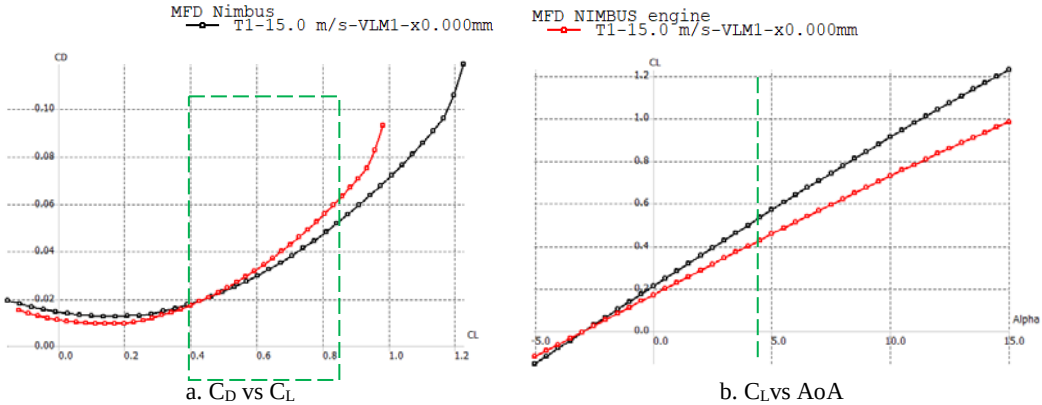

a. C_D vs C_L b. $C_L$vs AoA

Fig. 8 MFD Nimbus polars (speed 15 m/s)

Figure 9a shows a decrease in longitudinal stability (C_m) but an increase in lift-to-drag ratio (C_L/C_D) depending on AoA, see Figure 9b due to the presence of engine nacelles.

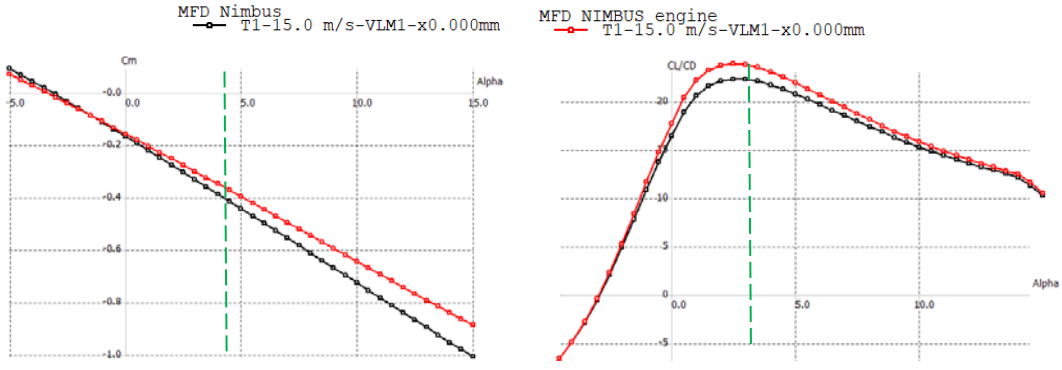

a. C_m vs AoA b. C_L/C_D vs AoA

Fig. 9 MFD Nimbus polars(speed 15 m/s)

The presence of nacelles, both depending on AoA (Figure 10a) and on C_L (Figure 10b), decreases the maximum endurance factor ($C_L^{3/2}/C_D$), according to the value of the corresponding lift coefficient AoA=4^0.

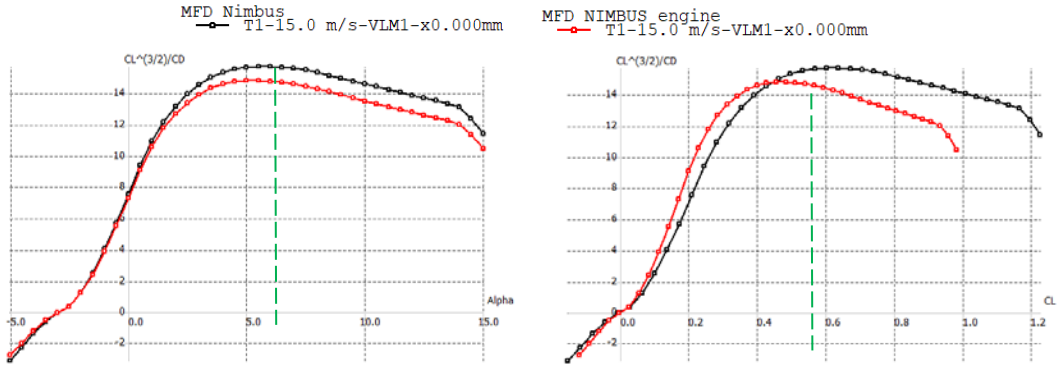

a. Power factor vs AoA b. Power factor vs C_l

Fig. 10 MFD Nimbus polars (speed 15 m/s)

The yawing (Figure 11a) and rolling coefficients (Figure 11b) are positively influenced by the presence of motor nacelles.

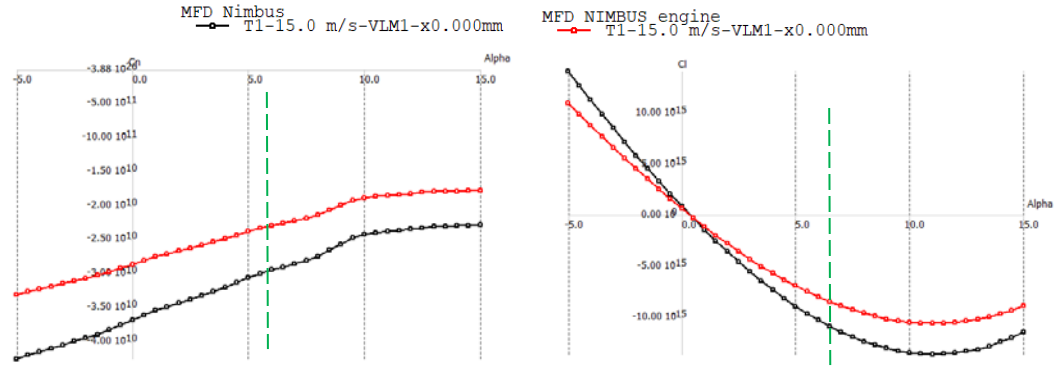

a. Yawing coefficient. vs AoA b. Rolling coefficient vs AoA

Fig. 11 MFD Nimbus polars (speed 15 m/s)

Figure 12 highlights the differences in variation of the balance (% of MAC) for the two geometric variants.

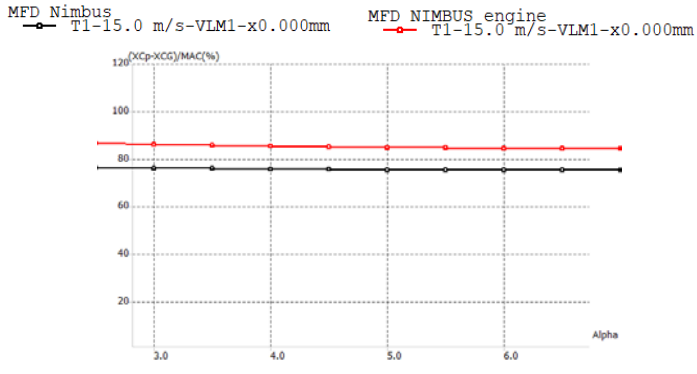

Fig. 12 Nimbus balance

According to Figure 13, it can be seen, as expected, the increase of the wing induced drag and viscous drag due to the presence of the engine nacelles.

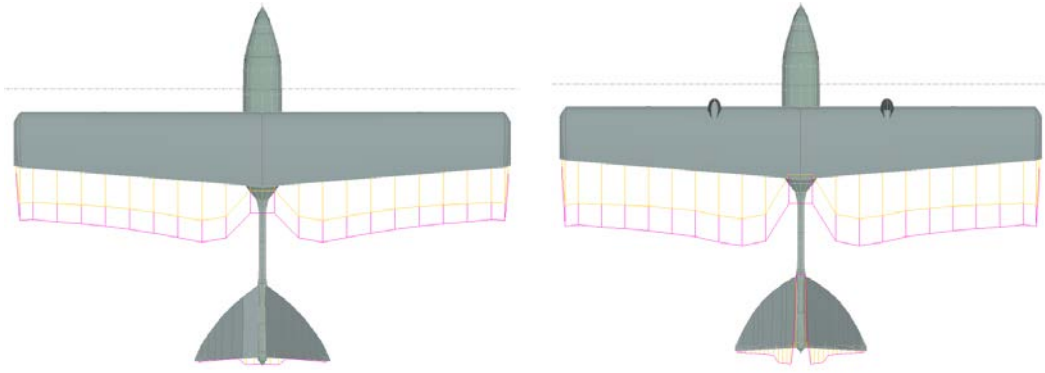

a b

Fig. 13 Induced drag and vâscous drag, MFD Nimbus (speed 15 m/s)

5. CONCLUSIONS

MFD Nimbus is an optimized aerodynamic UAV for FPV flights with a self-stabilized wing and large V-well to minimize mass and a good response to the manoeuvring, although no inertial data was used in aerodynamic analyses. The presence of engine nacelles significantly influences global aerodynamics.

The article highlights the influence of engine nacelles on the overall aerodynamic performance of the UAVs under the use of a freeware tool. Aerodynamic analyzes performed with freeware tools can generate results that are influenced by 2D and 3D geometry fidelity, the use of initial analysis conditions and geometric limitations. Numerical simulations on the proposed UAV have been limited which has led to the strict choice of initial simulation conditions with minimal implications for the level of confidence of the results.

In the next steps, dynamic UAV analysis will be resumed, including approaches to manoeuvring qualities by parameterization control surfaces (elevon, elevator) under real-life inertial values.

ACKNOWLEDGMENT

This article was produced with the support of the documentation of the complex project, acronym MultiMonD2, code PNIII-P1-1.2-PCDDI-2017-0637, contract 33PCCDI/ 2018 funded by UEFISCDI.

REFERENCES

[1] * * * MFD Nimbus, available at https://www.fpvmodel.com/myflydream-mfd-nimbus-1800-long-range-rc-fpv-plane-kit-only_g1273.html, accessed at 12.03.2019.

[2] V. Prisacariu, L. Simionescu, *Flight performance analysis for UAVs. MFD NIMBUS*, Scientific research and education in the Air Force – AFASES 2018, ISSN, ISSN-L: 2247-3173, p. 225-232, DOI: 10.19062/2247-3173.

[3] M. Drela, H. Yungren, *Guidelines for XFLR5 v6.03 (Analysis of foils and wings operating at low Reynolds numbers)*, 2011, available at http://sourceforge.net/projects/xflr5/files, accessed at 12.03.2019.

[4] * * * http://airfoiltools.com/airfoil/details?airfoil=clarkysm-il, accessed at 12.03.2019.

[5] C. A. Lyon, A. P. Broeren, P. Giguère, A. Gopalarathnam, and M. S. Selig, *Summary of Low-Speed Airfoil Data*, Volume **3**, SoarTech Publications Virginia Beach, Virginia, 1997, ISBN 0-9646747-3-4.

[6] V. Prisacariu, M. Boşcoianu, I. Cîrciu, Management of robotic aerial systems accomplishment, *RECENT Journal* **2**/2012, Transilvania University of Brasov, Romania, ISSN 1582-0246, p. 203-217.
[7] J. D. Anderson, Jr., *Fundamentals of Aerodynamics*, Fourth Edition, McGrawHill, New York, USA, 2007.
[8] M. Willner, *A Tutorial of XFLR version 1*, available at http://www.v0id.at/downloads/XFLR5-tut-v1.pdf accessed at 24.03.2019.
[9] D. Selig, F. Selig, *Airfoil at low speed*, publisher H.A. Stokely, USA, 1989, 408p, available at www.m-selig.ae.illinois.edu/uiuc_lsat/Airfoils-at-Low-Speeds.pdf.
[10] V. Prisacariu, CFD Analysis of UAV Flying Wing, *INCAS BULLETIN*, vol. **8**, issue 3, ISSN 2066 – 8201, DOI: 10.13111/2066-8201.2016.8.3.6, p 65-72, 2016.
[11] J. F. Marchman III, T. D. Werme, *Clark Y at low Reynolds Number*, AIAA 22nd Aerospace Science Meeting, 1984, http://user.engineering.uiowa.edu/~me_160/CFD%20Labs_/Lab2/clark-y-paper.pdf, accessed at 24.03.2019.
[12] C. A. Lyon, A. P. Broeren, P. Giguere, A. Gopalarathnam, and M. S. Selig, *Summary of Low-Speed Airfoil Data*, vol. 3, SoarTech Publications Virginia Beach, Virginia, ISBN 0-9646747-3-4, 1997, available at https://m-selig.ae.illinois.edu/uiuc_lsat/Low-Speed-Airfoil-Data-V3.pdf